CHAPTER

High-speed operation of alternating current motors

8

In variable speed drive applications such as alternating current (AC) servo and traction drive systems, a high-speed operation capability as well as a fast torque response of motors are needed. For example, for spindle drives in machine tools, a high-speed operation of more than several 10,000 r/min is required for enhancing cutting efficiency and accuracy. Traction drives such as electric cars, electric trains, electric forklifts, and dehydration of washing machines also require a high-speed operation of several times the rated speed. In addition, motors for driving compressors or motors for driving a torpedo and a missile need to be operated at a high-speed region of several 10,000 r/min. In this chapter, we will discuss the high-speed operation of AC motors. We introduce the field-weakening methods, which achieve the maximum torque capability of motors as well as a high-speed operation.

In the variable speed drives, the voltage applied to the motor should be increased with the operating speed. This is to maintain the current needed for the torque production of the motor. Since the back-EMF increases with the operating speed, the motor voltage should also be increased to control the current properly. As the speed increases, the motor reaches a speed (commonly called *base speed*) at which the applied motor voltage is equal to its rated value. From this speed, since the motor voltage is fixed at the rated voltage, we need to limit the back-EMF to a suitable level despite the increase in the speed.

For this purpose, a field-weakening control to reduce the field flux of the motor is necessary. As can be seen from Chapter 2 and Chapter 3, the back-EMF of direct current (DC) motors and AC motors is directly proportional to the operating speed ω_m (or frequency f) and the field flux as

$$E_{DC} \propto \phi \cdot \omega_m \quad \text{or} \quad E_{AC} \propto \phi \cdot f \tag{8.1}$$

If the field flux of a motor decreases with the increased speed, then the back-EMF is limited to a suitable level. Thus the voltage margin to control the current correctly can be maintained.

As an example, consider a high-speed operation in the DC motor drives. First, we will assume that the field flux ϕ is constant and the torque production to drive

Electric Motor Control. DOI: http://dx.doi.org/10.1016/B978-0-12-812138-2.00008-8

a load requires an armature current I_a. From the voltage equation of Eq. (2.1), the armature current in the steady-state is given as

$$I_a = \frac{V_a - E_a}{R_a} = \frac{V_a - k_e \phi \omega_m}{R_a} \tag{8.2}$$

Since the back-EMF increases as the operating speed increases, the armature voltage V_a applied to the motor should be increased with the increase in the speed to achieve the required current I_a. However, there is a limitation to the voltage applied to the motor because the motor voltage should not be greater than the rated voltage. Therefore the motor voltage required to regulate the command current may be insufficient in the high-speed region. As shown in Fig. 8.1, when the back-EMF is close to the full voltage of the motor as the speed increases, the current (thus output torque) of the motor is decreased rapidly. As a result, the speed no longer increases.

However, as shown in Fig. 8.2, if we limit the back-EMF to a constant value over the high-speed region by using the field-weakening control, which reduces the field flux in proportion to the inverse of the speed, then the voltage margin that regulates the current can be maintained and the output torque can be developed adequately. As a result, the speed of the motor can increase more than the rated speed.

For DC motors, the back-EMF can easily be maintained at a constant by reducing the field flux in proportion to the inverse of the speed so that the high-speed operation can function properly. However, the high-speed operation of AC motors cannot be achieved by such a simple method, and the high-speed

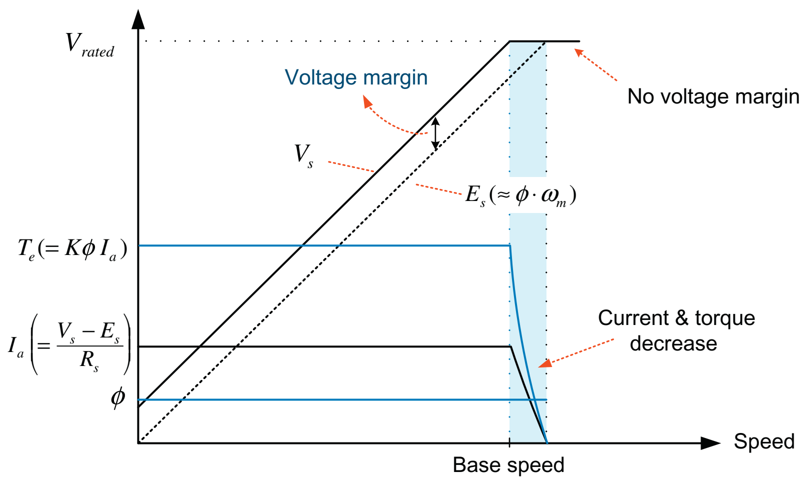

FIGURE 8.1

Motor characteristics according to speed (without field-weakening control).

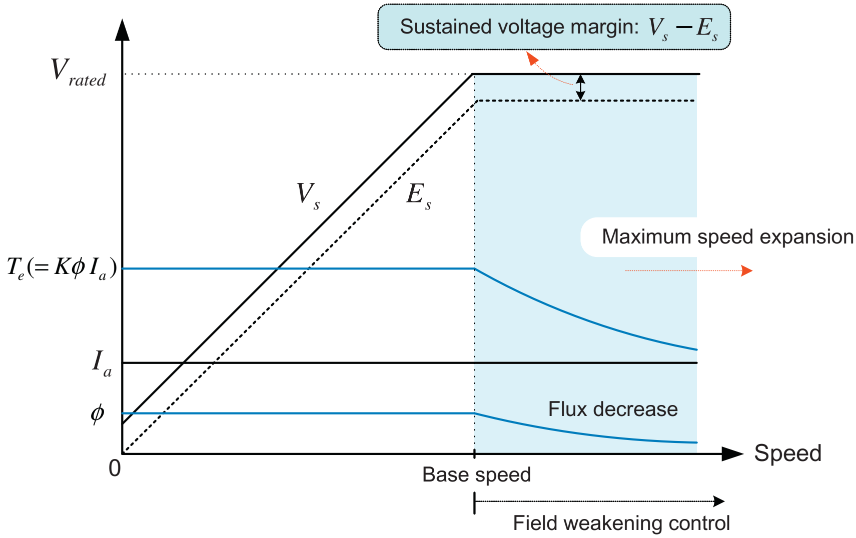

FIGURE 8.2

Motor characteristics according to speed (with field-weakening control).

operation method is different depending on the type of AC motor. Now we will discuss the field-weakening method for the high-speed operation of vector-controlled AC motors. We will start with an induction motor.

8.1 FIELD-WEAKENING CONTROL FOR INDUCTION MOTORS [1,2]

Induction motors are beneficial for high-speed operations due to their mechanical robustness. In addition, the output torque characteristic of induction motors in the constant power region matches well with a load (i.e., load torque inversely proportional to speed) requiring high-speed operation. Moreover, since the field flux of the vector-controlled induction motor can be easily weakened by reducing the d-axis current as the rotor speed increases, high-speed operations can be done easily. However, even though the same voltage and current are used, the developed torque capability of the motor at high speeds can vary according to the applied field-weakening strategy.

The field-weakening control method for induction motors can be classified into two methods: the *feedforward method* [1], which derives the flux command required for high-speed operation from the steady-state voltage equations of an induction motor, and the *feedback method* [2], which obtains the flux command from the voltage feedback. Now we will discuss the feedforward field-weakening control method in the vector control based on the rotor flux of induction motors.

8.1.1 CLASSIC FIELD-WEAKENING CONTROL METHOD

The method that was previously used for the field-weakening operation of induction motors was to simply vary the flux-producing current, i.e., d-axis stator current i_{ds}^{e} in proportion to the inverse of the rotor speed ω_r in the same way for DC motors as

$$i_{ds}^{e*} = \frac{\omega_{r\text{-}base}}{\omega_r} \cdot I_{d\text{-}rated} \tag{8.3}$$

where $I_{d\text{-}rated}$ is the rated d-axis current and $\omega_{r\text{-}base}$ is the base speed.

From this d-axis current command, the rotor flux command according to the speed in the field-weakening region is given as

$$\lambda_{dr}^{e*} = L_m i_{ds}^{e*} = L_m \left(\frac{\omega_{r\text{-}base}}{\omega_r} \right) \cdot I_{d\text{-}rated} \tag{8.4}$$

However, the flux command λ_{dr}^{e*} given by Eq. (8.4) cannot properly retain the voltage margin required for current control in the high-speed region. This is because the command flux level is too high to reduce the back-EMF appropriately. As a result, it is impossible to regulate the current commands required to perform the vector control properly, and thus the output torque capability of the induction motor is degraded. Moreover, the drive system may even fail to operate.

In Ref. [1], the authors introduced the optimal field-weakening method, which achieve the maximum torque capability of the induction motor and the high-speed operation. Now we will discuss this feedforward field-weakening method in more detail.

Since the developed torque of a motor depends on the available voltage and current, we need to begin with investigating the range of voltage and current available for an induction motor. The voltage applied to the motor is never greater than the rated value. On the other hand, the current often has a short-time rating, being two to three times greater than the rated current for a high-acceleration/high-deceleration torque production. Therefore we need to consider the available motor voltage and current for deriving the effective field-weakening method.

8.1.2 VOLTAGE- AND CURRENT-LIMIT CONDITIONS

In this section, we will examine the boundary of the current available for the torque production of an induction motor. This boundary can be obtained from the available voltage and current as follows.

8.1.2.1 *Voltage-limit condition*

For an inverter-driven motor, the motor voltage is supplied by an inverter. The maximum output voltage $V_{s\,max}$ of an inverter is determined by the available DC input voltage V_{dc}. Even under the same DC voltage, the maximum output voltage depends on the pulse width modulation (PWM) technique used. For example, as stated in Chapter 7, the space vector pulse width modulation (SVPWM) technique can produce a maximum voltage of $V_{dc}/\sqrt{3}$, while the sinusoidal pulse width modulation (SPWM) technique can produce that of $V_{dc}/2$.

For the maximum voltage $V_{s\,max}$ of a motor, the $d-q$ axes stator voltages should always satisfy the following relation.

$$v_{ds}^2 + v_{qs}^2 \le V_{s\,max}^2 \tag{8.5}$$

This is called *voltage-limit condition*. Here, the selection of the value of the maximum phase voltage $V_{s\,max}$ has a strong influence on the field-weakening operation performance. Considering the voltage drops of the switching devices, dead-time effects, and control stability, it is desirable to set this value at 90–95% of the maximum attainable voltage by a PWM technique in an inverter. If the value of $V_{s\,max}$ is inappropriately selected, then it can cause degradation or even a failure of high-speed operations.

The synchronous $d-q$ axes voltage equations of a vector-controlled induction motor based on the rotor flux are rewritten from Eqs. (6.16) and (6.17) as

$$v_{ds}^e = R_s i_{ds}^e + p\left(\sigma L_s i_{ds}^e + \frac{L_m}{L_r}\lambda_{dr}^e\right) - \omega_e \sigma L_s i_{qs}^e \tag{8.6}$$

$$v_{qs}^e = R_s i_{qs}^e + p\sigma L_s i_{qs}^e + \omega_e\left(\sigma L_s i_{ds}^e + \frac{L_m}{L_r}\lambda_{dr}^e\right) \tag{8.7}$$

When considering high-speed operations, the voltage drops on the stator resistance is negligible compared to the back-EMFs, so the above equations can be simplified in the steady-state as

$$v_{ds}^e \approx -\omega_e \sigma L_s i_{qs}^e \tag{8.8}$$

$$v_{qs}^e \approx \omega_e\left(\sigma L_s i_{ds}^e + \frac{L_m}{L_r}\lambda_{dr}^e\right) \approx \omega_e L_s i_{ds}^e \tag{8.9}$$

By substituting these equations into Eq. (8.5), the voltage-limit condition can be expressed in terms of $d-q$ axes stator currents as

$$\left(\omega_e \sigma L_s i_{qs}^e\right)^2 + \left(\omega_e L_s i_{ds}^e\right)^2 \le V_{s\,max}^2 \tag{8.10}$$

This expression illustrates the boundary of the controllable $d-q$ axes currents by using the maximum available voltage $V_{s\,max}$. This voltage-limit boundary is expressed as an ellipse equation, which is a function of operating frequency ω_e as shown in Fig. 8.3. The inside of the ellipse indicates the controllable current region. Any $d-q$ current command inside the ellipse is controllable by using the given voltage $V_{s\,max}$. Thus the current commands should remain inside the voltage-limit ellipse given at each operating frequency. The radius of the ellipse becomes smaller as the operating frequency increases. This means that, under a given voltage, the boundary of controllable currents becomes smaller. This is because the back-EMF increases as the operating frequency increases. Unlike DC

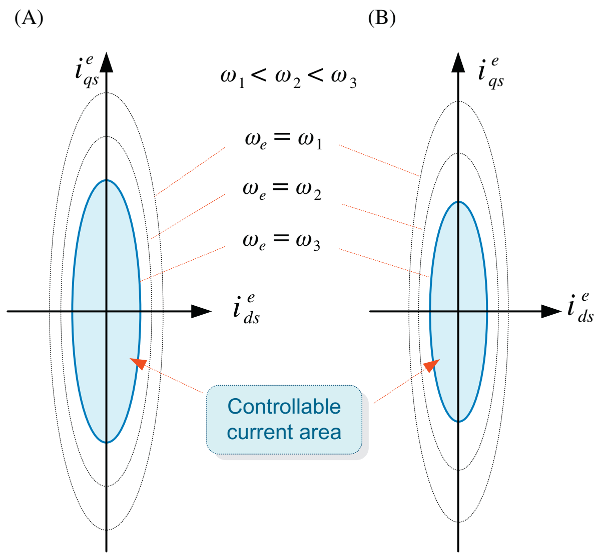

FIGURE 8.3

Voltage-limit condition. (A) Small leakage factor and (B) large leakage factor.

motors, the back-EMF of induction motors increases with the operating frequency rather than the rotor speed.

Fig. 8.3A and B shows several ellipses for different operating frequencies. We can see from Eq. (8.10) that the leakage inductance (or leakage factor σ) has a significant influence on the shape of the ellipse at a specific operation frequency. The area of the ellipse is smaller for an induction motor with a large leakage factor as in Fig. 8.2B than for one with a small leakage factor as in Fig. 8.2A at the same operating frequency. This implies that for an induction motor with a large leakage factor, more voltage is necessary for regulating an equal value of current commands. As stated in Chapter 3, an induction motor with a large leakage factor has a narrow range of the constant power region. This is because the leakage factor has an influence on the maximum values of the slip. Fig. 8.3 explains this phenomenon. Hence, the leakage factor is an important factor in the design of an induction motor.

Next, we will discuss the current-limit condition for a motor.

8.1.2.2 Current-limit condition

The motor current is usually limited by the rated current. A 150–300% rated current, however, is often allowed for a short period of time to produce a high-acceleration/high-deceleration torque, given that it does not exceed the motor thermal rating. The current rating of an inverter should be selected so that it can provide the maximum motor current.

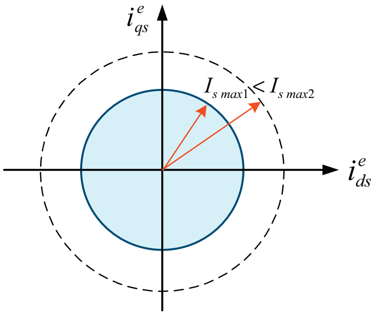

FIGURE 8.4

Current-limit condition.

Under the maximum available stator current $I_{s\,max}$, the $d-q$ axes stator currents of an induction motor are restricted to the following condition.

$$i_{ds}^2 + i_{qs}^2 \le I_{s\,max}^2 \tag{8.11}$$

This is referred to as *current-limit condition*. This current-limit boundary can be expressed as a circle in the $d-q$ axes current plane as shown in Fig. 8.4, whose radius is the maximum stator current $I_{s\,max}$. To satisfy this current-limit condition, the $d-q$ axes stator current commands should always be inside this circle. Unlike the voltage-limit condition, the boundary of the current-limit condition remains constant regardless of the operating frequency.

When we drive an induction motor, the two conditions of the voltage- and current-limit should be always satisfied. Considering both the voltage- and the current-limit conditions, the region of the controllable currents is the common area between the current-limit circle and the voltage-limit ellipse for a given operating frequency, which is the *dark area* shown in Fig. 8.5.

Thus the $d-q$ axes stator current commands in the induction motor drive must be inside this area for a given operating frequency.

Now we will find out the optimal flux under the voltage- and the current-limit conditions for the field-weakening control, which can obtain the maximum output torque capability of an induction motor over the whole high-speed region.

8.1.3 FIELD-WEAKENING CONTROL FOR PRODUCING THE MAXIMUM TORQUE

In a vector-controlled induction motor, the output torque can be expressed as a function of $d-q$ axes stator currents as

$$T_e = \frac{3}{2}\frac{P}{2}\frac{L_m^2}{L_r} i_{ds}^e i_{qs}^e = k i_{ds}^e i_{qs}^e \quad \left(k = \frac{3}{2}\frac{P}{2}\frac{L_m^2}{L_r}\right) \tag{8.12}$$

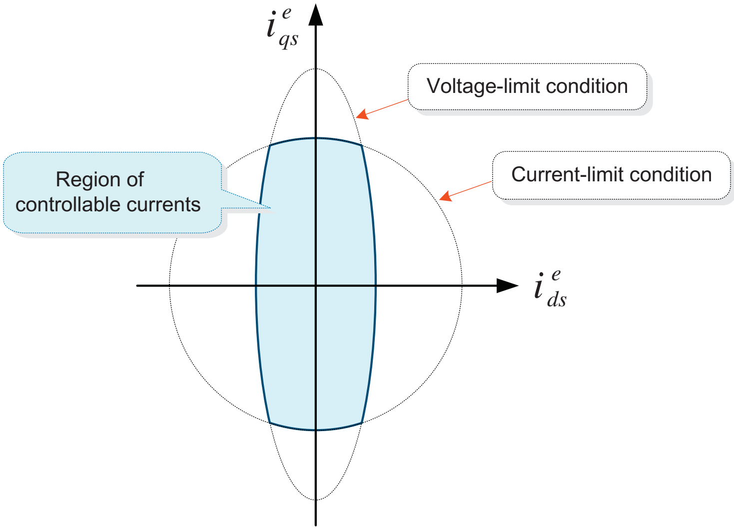

FIGURE 8.5

Region of controllable currents for voltage- and current-limit conditions.

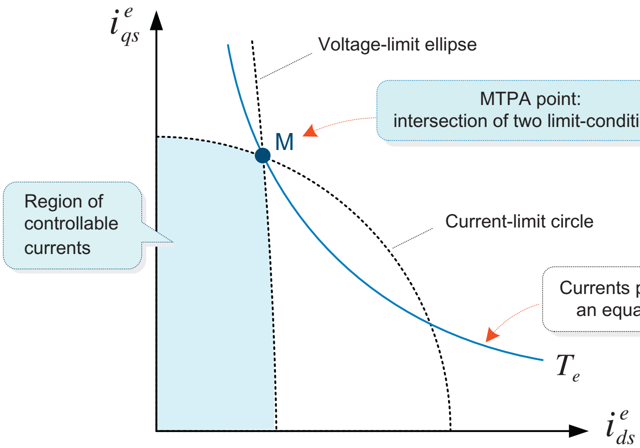

FIGURE 8.6

Voltage- and current-limit conditions and MTPA point.

The value of the output torque varies according to the chosen combinations of d–q axes stator currents, i_{ds}^e and i_{qs}^e. Fig. 8.6 illustrates numerous combinations of the stator currents to produce an equal output torque, along with the voltage- and the current-limit conditions. Here, we will consider only Quadrant 1, which indicates the motoring operation mode for the forward driving.

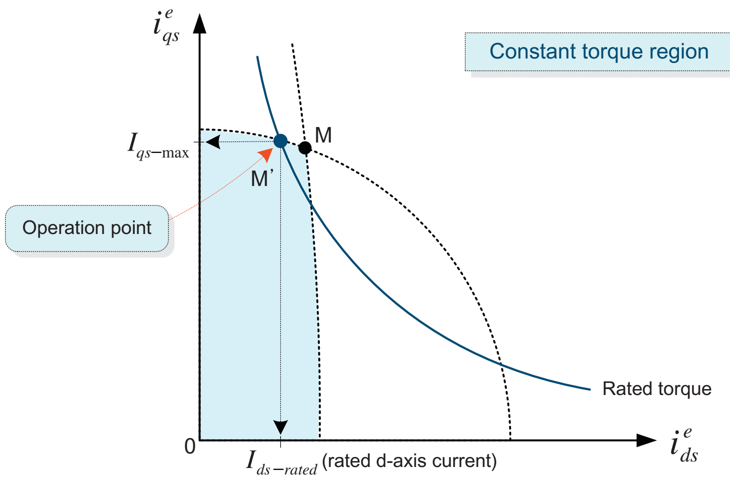

FIGURE 8.7

Optimal operating point in the constant torque region.

In the available region under both the voltage- and current-limit conditions, the optimal current combination maximizing the output torque becomes the value at the intersection (M point) of the circle and the ellipse at a given operating frequency. This operating point indicates the minimum stator current for producing the required torque. Thus this is the *maximum torque per ampere* (MTPA) operating point. This optimal operating point varies according to the operating speed, and it can be obtained as follows.

8.1.3.1 Constant torque region ($\omega_e \leq \omega_{base}$)

In the low- and mid-speed range, the d-axis stator current at the optimal operating point M is usually greater than rated d-axis current $I_{ds\text{-}rated}$ for producing the rated rotor flux linkage $\lambda_{dr\text{-}rated}^{e}$ as shown in Fig. 8.7. Even if the d-axis current is increased above the rated value, the flux level does not increase accordingly because of the saturation of the iron core. For this reason, in this speed range, the d-axis stator current command (thus, rotor flux command) is maintained at the rated value as

$$i_{ds}^{e*} = I_{ds\text{-}rated} \tag{8.13}$$

$$\lambda_{dr}^{e*} = \lambda_{dr\text{-}rated}^{e} = L_m i_{ds}^{e*} = L_m I_{ds\text{-}rated} \tag{8.14}$$

In this case, the available output torque depends only on the available q-axis stator current. The available q-axis stator current is limited by the d-axis current command as

$$i_{qs\text{-}max}^{e*} = \sqrt{I_{s\ max}^{2} - i_{ds}^{e*2}} = \sqrt{I_{s\ max}^{2} - I_{ds\text{-}rated}^{2}} \tag{8.15}$$

Thus, in this speed range, the operating point is given as M′ point as shown in Fig. 8.7. This condition is still held at operating speeds below the rated speed (more accurately, the base speed).

Next, we will examine the optimal flux for producing the maximum torque in the high-speed range. The high-speed region, which is called *field-weakening region*, has two subregions as follows.

8.1.3.2 Constant power region ($\omega_{base} \le \omega_e < \omega_{BT}$): Field-weakening region I

In the constant torque region as stated earlier, when the operating frequency is increased, the boundary of the voltage-limit ellipse will be reduced. This indicates that, due to a limited $V_{s\,max}$, the controllable current region is reduced as the back-EMF increases with the operating frequency.

Even though the voltage-limit ellipse is reduced by the increase in operating frequency, the rated *d*-axis current can still be used, provided that the controllable current region includes the rated *d*-axis current. As the operating frequency is further increased, the *d*-axis stator current at the intersection of the circle and ellipse will coincide with the rated *d*-axis current as shown in Fig. 8.8. The operating frequency at this moment is the onset frequency at which the constant power region begins. The speed at this onset frequency is called the *base speed* ω_{base}. For the operation above the base speed, the *d*-axis stator current should be lowered below the rated *d*-axis current. In other words, the field-weakening operation should start reducing the flux level.

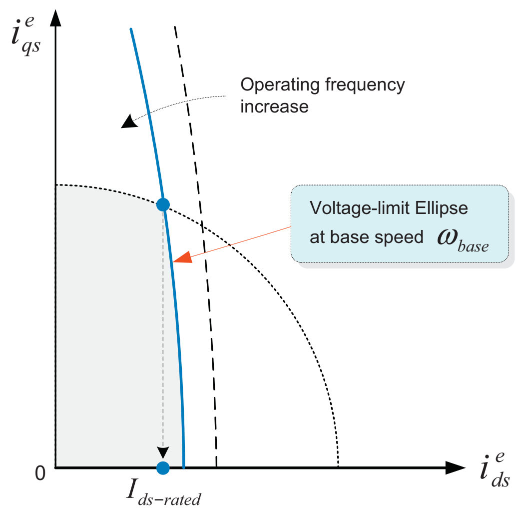

FIGURE 8.8

Onset of field-weakening operation.

From Eqs. (8.10) and (8.11), the base speed is given as

$$\omega_{base} = \frac{\sqrt{V_{s\,max}^2[(L_sI_d)^2+(\sigma L_sI_q)^2]^2+[R_sI_dI_q(L_s-\sigma L_s)]^2}-R_sI_dI_q(L_s-\sigma L_s)}{(L_sI_d)^2+(\sigma L_sI_q)^2} \tag{8.16}$$

here, $I_d = I_{ds\text{-}rated}$ and $I_q = \sqrt{I_{s\,max}^2 - I_d^2}$ are the $d-q$ axes stator currents used in the constant torque region, respectively.

The base speed depends heavily on the motor parameters, and thus, varies with motors. Even for the same motor, the base speed varies according to the flux level used in the constant torque region and the available stator voltage and current. A higher flux level, low $V_{s\,max}$, or high $I_{s\,max}$ results in a lower base speed, and thus in such cases, the field-weakening operation should start at a lower speed.

From the base speed and the slip frequency, the base rotor speed is obtained by

$$\omega_{r\text{-}base} = \omega_e - \omega_{sl} \tag{8.17}$$

This base rotor speed may be different from the rated rotor speed according to operating conditions.

In this field-weakening region, the optimal current combination (i.e., optimal current vector) producing the maximum output torque is always given as the value at the intersection (M point) of the circle and ellipse. The optimal current vector moves along the current-limit boundary as shown in Fig. 8.9 because the voltage-limit ellipse dwindles as the operating frequency increases. This means that the d-axis stator current, and thus the rotor flux linkage λ_{dr}^e should be reduced as the operating frequency increases.

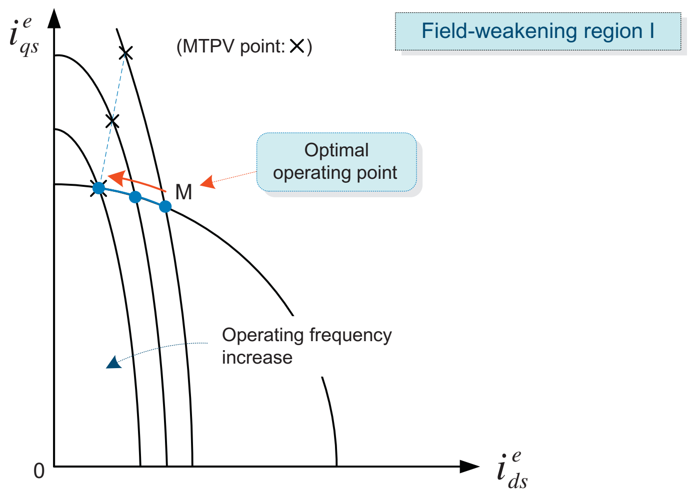

FIGURE 8.9

Optimal current trajectory in the field-weakening region I.

The d-axis stator current at this optimal point can be derived from the voltage- and current- limit conditions as

$$i_{ds}^{e} = \sqrt{\frac{\left(\frac{V_{s\,max}}{\omega_e}\right)^2 - (\sigma L_s I_{s\,max})^2}{L_s^2(1-\sigma)}} \tag{8.18}$$

In this case, the available maximum q-axis stator current can be increased by the decreasing amount of the d-axis current to use the allowable stator current $I_{s\,max}$ fully as

$$i_{qs\text{-}max}^{e} = \sqrt{I_{s\,max}^2 - i_{ds}^{e*2}} \tag{8.19}$$

From the optimal d-axis stator current, the optimal rotor flux command is given as

$$\lambda_{dr}^{e*} = L_m i_{ds}^{e*} = L_m \sqrt{\frac{\left(\frac{V_{s\,max}}{\omega_e}\right)^2 - (\sigma L_s I_{s\,max})^2}{L_s^2(1-\sigma)}} \tag{8.20}$$

It is important to note that the magnetizing inductance L_m varies due to the flux reduction in this region. Thus the optimal flux should be obtained by considering this inductance variation. Also, as stated in Chapter 5, since the relation between the d-axis stator currents i_{ds}^{e} and the rotor flux linkage λ_{dr}^{e} is a first-order lag, a flux controller should be used to control the flux accurately for an effective field-weakening operation.

In this region the stator voltage and current are maintained at a constant as $V_{s\,max}$ and $I_{s\,max}$, respectively. Thus this region is referred to as *constant power (constant VA) region*. In this region, as we can see from the slip equation of Eq. (5.32), the slip frequency increases as the operating frequency increases because the d-axis stator current decreases and the q-axis stator current increases. As the operating frequency is further increased, the slip frequency reaches its maximum value, and then the field-weakening region II begins.

8.1.3.3 Breakdown torque region ($\omega_e > \omega_{BT}$): Field-weakening region II

As the operating frequency is further increased in the field-weakening region I, the voltage-limit ellipse will be reduced further, and a large portion will be included in the current-limit circle as shown in Fig. 8.10. This implies that the voltage-limit condition is included in the current-limit condition.

Furthermore, if the optimal current for producing the maximum torque subject to only the voltage-limit condition (point X on the voltage-limit ellipse) is included inside the current-limit circle, we can consider only the voltage-limit condition for obtaining the optimal flux. This situation corresponds to *field-weakening region II*. This optimal point subject to only the voltage-limit condition is called the *maximum torque per voltage* (MTPV) operating point.

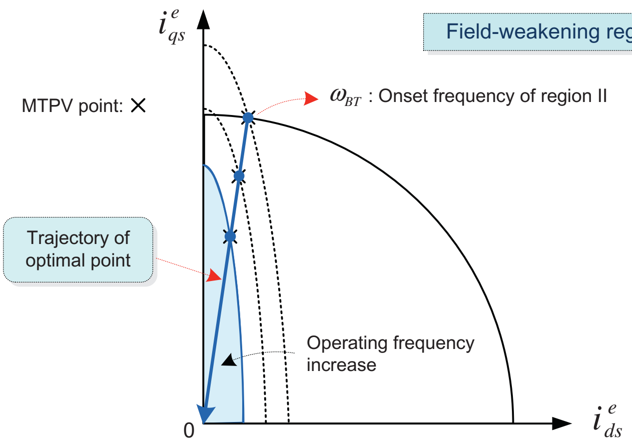

FIGURE 8.10

Maximum torque operation point for the field-weakening region II.

The onset speed of the field-weakening region II is the frequency ω_{BT}, at which the optimal current vector for the MTPV operation is just on the circumference of the current-limit circle, and can be given as

$$\omega_{BT} = \sqrt{\frac{1+\sigma^2}{2(\sigma L_s)^2}} \times \left(\frac{V_{s\,max}}{I_{s\,max}}\right) \tag{8.21}$$

This onset frequency ω_{BT} depends on the leakage inductance as well as the maximum values of the voltage and current. Induction motors with a large leakage factor will begin the operation of the field-weakening region II at a lower speed. Thus they have a narrow range of the constant power region.

In this field-weakening region II, the optimal stator currents for producing the maximum torque are given as

$$i_{ds}^{e} = \frac{V_{s\,max}}{\sqrt{2}\omega_e L_s} \tag{8.22}$$

$$i_{qs}^{e} = \frac{V_{s\,max}}{\sqrt{2}\omega_e \sigma L_s} \tag{8.23}$$

From the optimal d-axis stator current, the optimal rotor flux command is given as

$$\lambda_{dr}^{e*} = L_m i_{ds}^{e*} = \frac{V_{s\,max} L_m}{\sqrt{2}\omega_e L_s} \tag{8.24}$$

In this region, the optimal stator vector moves into the origin as the frequency increases as shown in Fig. 8.10. Thus, unlike the field-weakening region I, i_{qs}^{e*} is

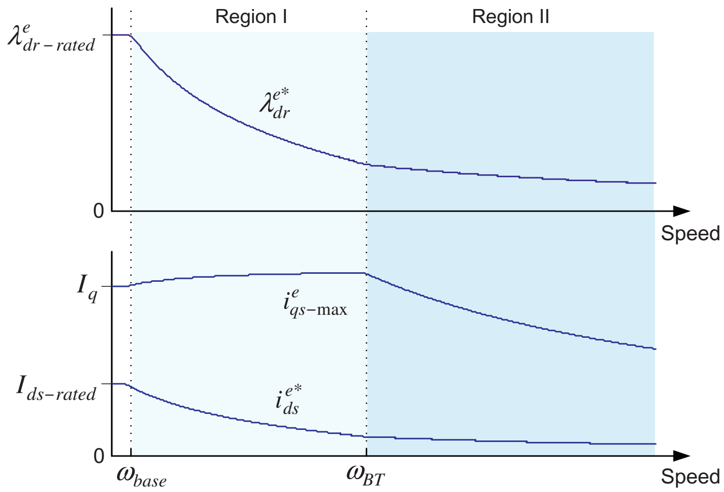

FIGURE 8.11

Optimal currents and flux in the field-weakening regions I and II.

also decreased along with the reduction of i^{e*}_{ds}. As a result, the total stator current will be reduced, and the output power will also be reduced. Fig. 8.11 shows the optimal $d-q$ currents and the rotor flux command according to the speed in the field-weakening regions I and II.

From the optimal $d-q$ axes currents of Eqs. (8.22) and (8.23), we can readily see that the slip frequency remains constant over this region as its maximum value, which is given as

$$\omega_{sl\text{-}max} = \frac{1}{T_r}\frac{i^e_{qs}}{i^e_{ds}} = \frac{1}{T_r\sigma} \tag{8.25}$$

The maximum torque developed by an induction motor in this region is quickly reduced by $1/\omega_e^2$ as

$$T_{e\text{-}max} = \frac{3}{2}\frac{P}{2}\frac{1}{2\sigma L_s^2}\left(\frac{V_{s\ max}}{\omega_e}\right)^2 \tag{8.26}$$

Fig. 8.12 compares the high-speed performance of the optimal field-weakening operation with that of the "$1/\omega_r$" method.

Since the level of the rotor flux command given at each operating frequency is inappropriate in the "$1/\omega_r$" method, the drive system does not exploit the output torque capability of the motor fully. Moreover, it will be hard to regulate the q-axis stator current command as the speed increases, so the vector control cannot be carried out in the high-speed region. As a result, the drive system will lose its controllability.

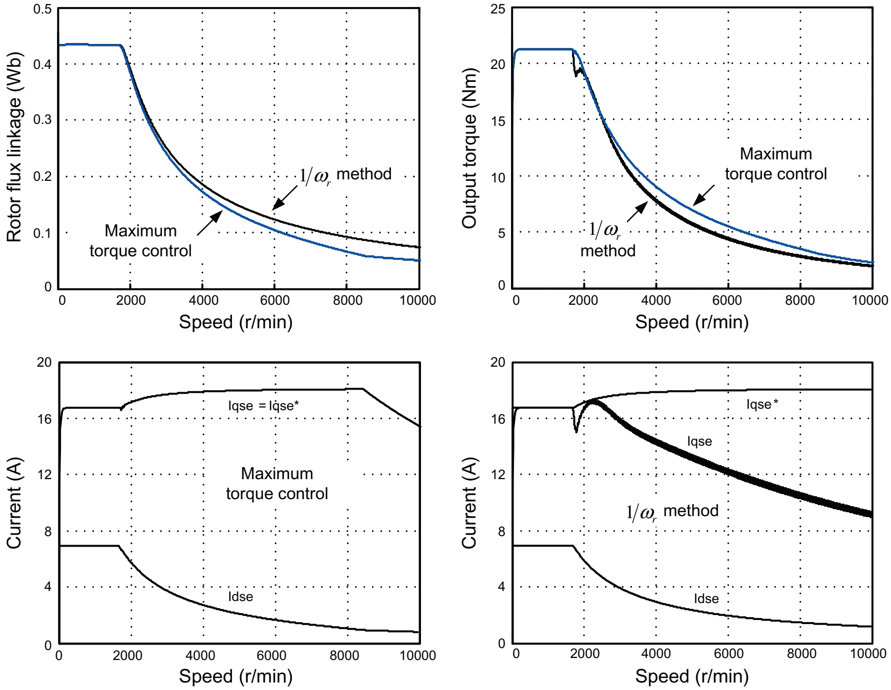

FIGURE 8.12

Comparison of the performance of the field-weakening methods (5-hp, 4-pole).

Fig. 8.13 shows a vector-controlled induction motor drive system with the field-weakening control for high-speed operations. The optimal flux reference can be given from Eq. (8.20) or (8.24) according to the operating speed.

Fig. 8.14 shows the experimental results on a 6-pole, 2.2-kW induction motor for the vector control system as shown in Fig. 8.13 [1]. The induction motor was accelerated up to 3000 r/min in the field-weakening region II by using the optimal strategy just described. The *d*-axis stator current is regulated to reduce the rotor flux according to the operating speed. Here, since the flux linkage is estimated by the voltage model, we can see that the estimated flux is inaccurate below the mid-speed range. While the *q*-axis current is increased in the field-weakening region I, it is decreased in the field-weakening region II.

To successfully carry out the optimal field-weakening operation, the optimal rotor flux reference at each operating frequency needs to be calculated correctly. In this feedforward field-weakening control method, the accuracy of the calculated optimal flux reference depends on the motor parameters such as the magnetizing inductance and leakage inductance. The magnetizing inductance will especially vary significantly due to the variation of the rotor flux level in the field-weakening operation. Therefore the variation of the magnetizing

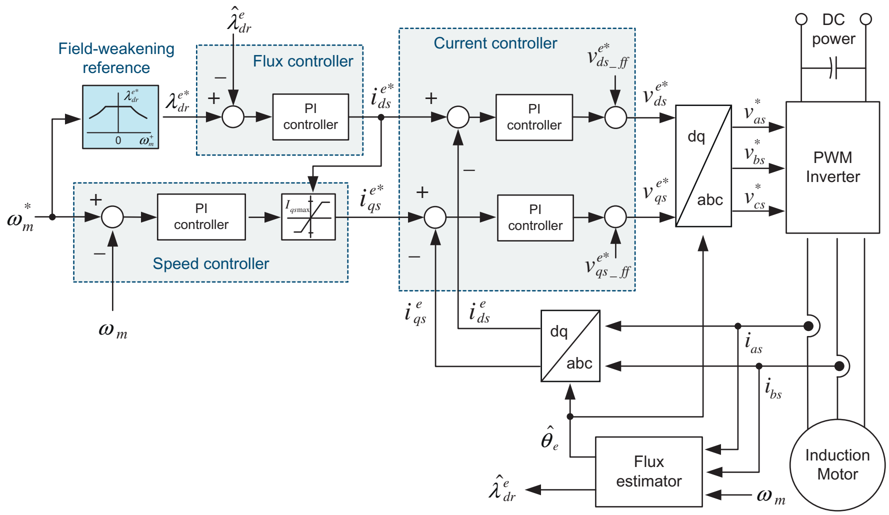

FIGURE 8.13

Vector control system of an induction motor with the field-weakening control.

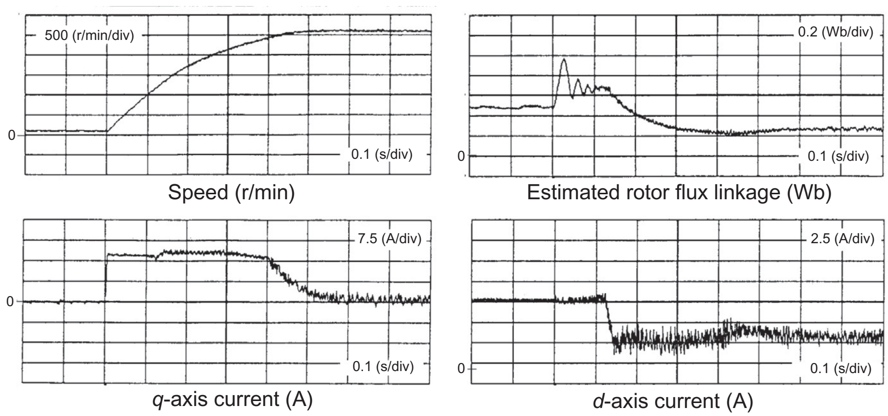

FIGURE 8.14

Optimal field-weakening operation (6-pole, 2.2-kW IM).

inductance should be considered. On the other hand, the leakage inductance is not dependent on the variation of the rotor flux level but on the magnitude of the stator current.

Unlike the feedforward field-weakening method sensitive to motor parameters, Kim and Sul [2] proposed another field-weakening control strategy that uses the feedback of the motor voltage without any motor parameter as shown

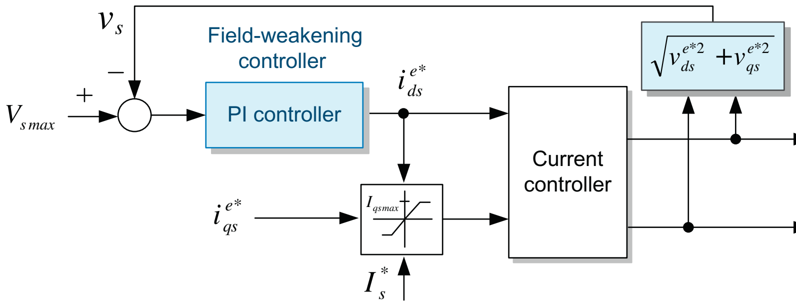

FIGURE 8.15

Field-weakening control strategy using the voltage feedback.

in Fig. 8.15. The feedback field-weakening control strategy is insensitive to motor parameters but cannot give dynamic response as fast as the feedforward strategy can.

The concept of the optimal field-weakening control methods of induction motors can be also used for high-speed operation of permanent magnet synchronous motors (PMSMs) as follows.

8.2 FLUX-WEAKENING CONTROL FOR PERMANENT MAGNET SYNCHRONOUS MOTORS [3–6]

As stated in Section 4.6, surface-mounted permanent magnet synchronous motors (SPMSMs) with magnets mounted on the surface of the rotor are unsuitable for high-speed operations with a higher centrifugal force. Furthermore, a reduction in stator inductance due to the magnets on the surface of the rotor hinders the flux-weakening operation, which reduces the magnet flux. On the contrary, interior permanent magnet synchronous motor (IPMSMs) are favorable for the high-speed operation since their magnets are inserted inside the rotor core and have a large inductance. For these reasons, IPMSMs are widely used for applications requiring a high-speed operation. Now we will discuss the flux-weakening control for the high-speed operation of PMSMs in more detail.

For motors such as an induction motor, separately excited DC motor, and synchronous motor with a field winding on the rotor, the field flux can be reduced directly by controlling the field current for high-speed operation. This technique is referred to as *field-weakening control*. By contrast, for PMSMs such as IPMSM or SPMSM, the field flux cannot be controlled directly because it is generated by a permanent magnet. As can be seen from Eq. (4.113), the stator flux linkage of PMSMs is given by

$$\lambda_{ds}^r = L_{ds} i_{ds}^r + \phi_f \tag{8.27}$$

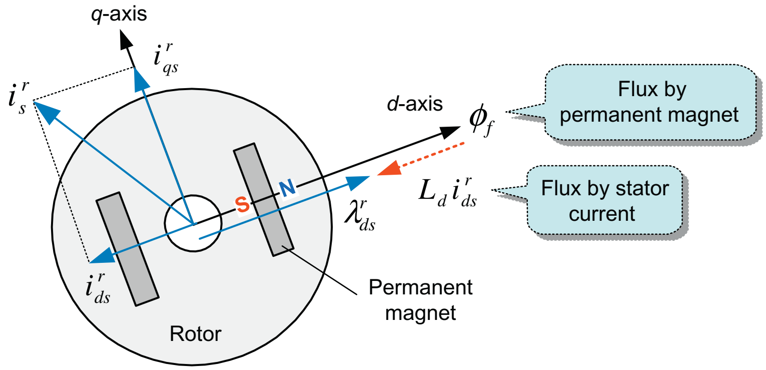

FIGURE 8.16

Concept of flux weakening.

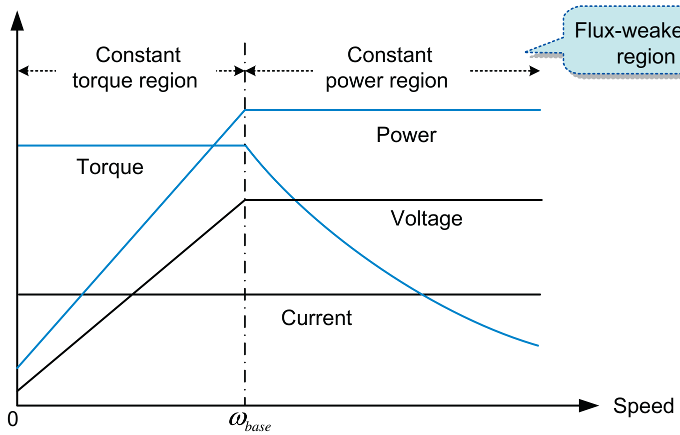

FIGURE 8.17

Operation region of PMSMs.

For PMSMs, if we produce the flux in the direction opposite of the magnet flux by using the negative *d*-axis stator current as shown in Fig. 8.16, we can reduce the effective stator flux linkage. This technique is referred to as *flux-weakening control*. From Eq. (8.27), we can see that a large *d*-axis inductance is desirable for an effective flux-weakening control.

The operation region of PMSMs can be normally divided into the following two speed regions.

- *Constant torque region*: Speed range below base speed
- *Constant power region*: Speed range above base speed (flux-weakening region)

Fig. 8.17 shows the characteristics in two speed regions.

The speed regions of PMSMs are basically similar to those of separately excited DC motors. However, PMSMs may have an additional flux-weakening region similar to the breakdown torque region of induction motors depending on their magnetic system design. This is determined by the magnitude relation between the magnet flux ϕ_f and the maximum d-axis stator flux linkage (i.e., $L_{ds}I_{s\,max}$). More practically, Fig. 8.18 shows the output power characteristics of the PMSMs according to the design. In the case of $\phi_f = L_{ds}I_{s\,max}$, PMSMs have a characteristic nearly similar to the ideal characteristic as shown in Fig. 8.17. The characteristics according to the magnetic system design will be explained in more detail in the Section 8.2.1.

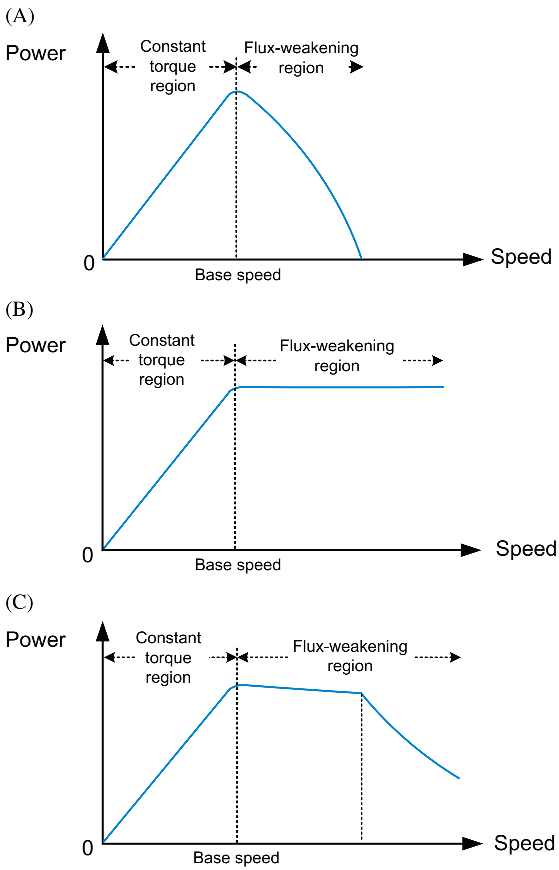

FIGURE 8.18

Output power according to speed regions of PMSM. (A) $\phi_f > L_{ds}I_{s\,max}$, (B) $\phi_f = L_{ds}I_{s\,max}$, and (C) $\phi_f < L_{ds}I_{s\,max}$.

The flux-weakening control techniques for the high-speed operation of PMSMs can be divided into three methods: *feedforward method*, which obtains the current commands required for the high-speed operation from steady-state voltage equations, *feedback method*, which obtains the current commands from the voltage feedback, and a *combined method* of these two techniques [3–5]. Here, we will explore the feedforward flux-weakening control method for IPMSMs and SPMSMs, separately.

8.2.1 HIGH-SPEED OPERATION OF AN INTERIOR PERMANENT MAGNET SYNCHRONOUS MOTOR

Before examining the high-speed operation of an IPMSM, we will first review the operation of an IPMSM in the constant torque region.

8.2.1.1 Constant torque region ($\omega_e \leq \omega_{base}$)

For the operation of an IPMSM in the constant torque region, which indicates an operating range below the base speed, the MTPA control is used as shown in Fig. 8.19.

In Section 5.5, we discussed how to obtain the optimal currents for MTPA operation. In the MTPA operation, the output torque of an IPMSM is mainly limited by only the maximum available stator current $I_{s\,max}$. However, for the high-speed range, where the back-EMF voltage becomes large, the voltage margin is insufficient to control the current commands for the MTPA operation. Thus the output torque of an IPMSM is limited by the available voltage rather than the available current.

Now we will examine the speed attainable under the maximum available stator voltage $V_{s\,max}$. In the vicinity of rated speed with a large back-EMF, since the

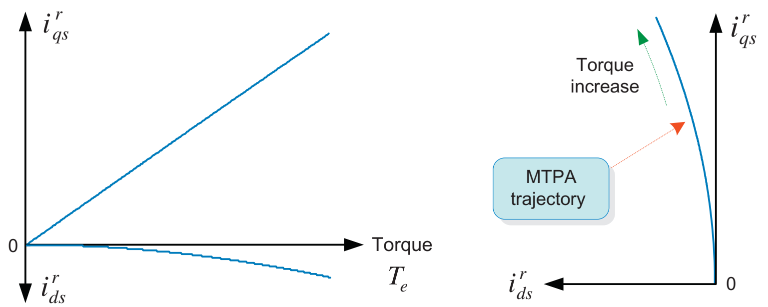

FIGURE 8.19

d–q axes current commands for MTPA operation.

voltage drops on the stator resistance is negligible, the $d-q$ axes stator voltages of an IPMSM in the steady-state are given from Eqs. (6.24) and (6.25) as

$$v_{ds}^r = -\omega_r L_{qs} i_{qs}^r \tag{8.28}$$

$$v_{qs}^r = \omega_r (L_{ds} i_{ds}^r + \phi_f) \tag{8.29}$$

These stator voltages should satisfy the following relation, which is the *voltage-limit condition* stated in Section 8.1.

$$v_{ds}^{r2} + v_{qs}^{r2} \leq V_{s\,max}^2 \tag{8.30}$$

From Eqs. (8.28)–(8.30), the maximum speed $\omega_{r\text{-}base}$ of the constant torque operation region can be obtained as

$$\omega_{r\text{-}base} = \frac{V_{s\,max}}{\sqrt{(L_{ds} I_{ds}^r + \phi_f)^2 + (L_{qs} I_{qs}^r)^2}} \tag{8.31}$$

where I_{ds}^r and I_{qs}^r are the $d-q$ axes currents used for MTPA operation, respectively.

The speed $\omega_{r\text{-}base}$ is the base speed at which the flux-weakening control should start for the constant power operation. The base speed varies with the required current (or torque) and the available voltage.

Next, we will discuss the flux-weakening control method in the constant power region.

8.2.1.2 Constant power region ($\omega_e > \omega_{base}$)

Similar to induction motors, the IPMSM operation is also confined to the voltage- and the current-limit conditions, which was explained in Section 8.1.2. Thus we need to find out the optimal flux-weakening control method that ensures a maximum torque production in the high-speed region under the voltage- and the current-limit conditions.

To begin with, we will express the voltage- and the current-limit boundaries for an IPMSM in the $d-q$ axes current plane. Similar to an induction motor, under the maximum available stator current $I_{s\,max}$, the $d-q$ axes stator currents of an IPMSM are restricted to the following condition.

$$i_{ds}^{r2} + i_{qs}^{r2} \leq I_{s\,max}^2 \tag{8.32}$$

The current-limit boundary in the $d-q$ axes currents plane is shown in Fig. 8.20. This current-limit boundary is expressed as a circle, whose radius is $I_{s\,max}$. On the other hand, the voltage-limit boundary can be expressed from Eqs. (8.28)–(8.30) as

$$(\omega_r L_{qs} i_{qs}^r)^2 + (\omega_r L_{ds} i_{ds}^r + \omega_r \phi_f)^2 \leq V_{s\,max}^2 \tag{8.33}$$

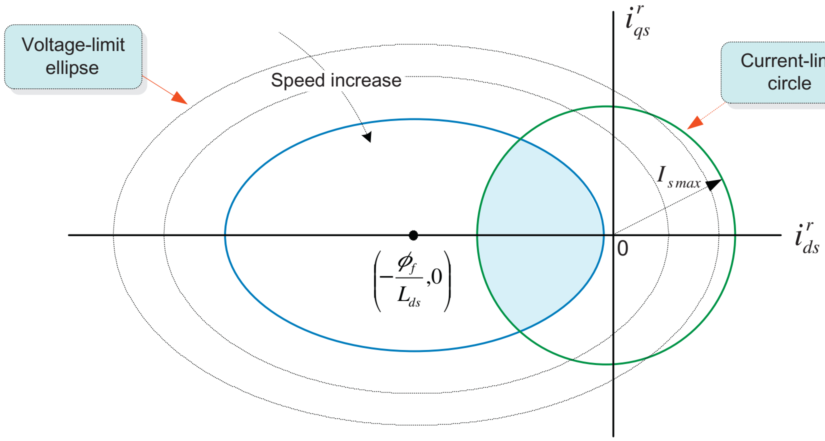

FIGURE 8.20

Voltage- and current-limit boundaries.

This voltage-limit boundary as shown in Fig. 8.20 is an ellipse equation, whose center is given as

$$(i_{ds0}^r, i_{qs0}^r) = \left(-\frac{\phi_f}{L_{ds}}, 0\right) \tag{8.34}$$

This expression illustrates the boundary of controllable $d-q$ axes currents by using the given maximum stator voltage $V_{s\,max}$. The inner region of the ellipse reduces as the operating speed ω_r increases. This indicates that the boundary of controllable currents becomes smaller as the operating speed increases. This is because the back-EMF increases as the operating speed increases.

The IPMSM drives should always satisfy both the voltage- and the current-limit conditions. Considering these two limit conditions, the region of controllable currents is the common area between the current-limit circle and the voltage-limit ellipse for a given operating speed, which is the *dark area* shown in Fig. 8.20. Thus the $d-q$ axes stator current commands must be inside this area for a given operating speed.

Now let us investigate the optimal operating point for producing the maximum output torque under these voltage- and current-limit conditions. For an IPMSM, as can be seen in Fig. 8.18, the maximum operating speed and the output power characteristic vary according to the magnitude relationship between the magnet flux ϕ_f and the maximum d-axis stator flux linkage (i.e., $L_{ds}I_{s\,max}$). This relationship can also be expressed by whether or not the center of the voltage-limit ellipse is inside the current-limit circle. According to this relationship, a different flux-weakening control strategy is required [6].

The maximum attainable operating speed of an IPMSM can be given by letting $i_{ds}^r = -I_{s\,max}$, $i_{qs}^r = 0$ in Eq. (8.31) as

$$\omega_{r\text{-}max} = \frac{V_{s\,max}}{\phi_f - L_{ds}I_{s\,max}} \tag{8.35}$$

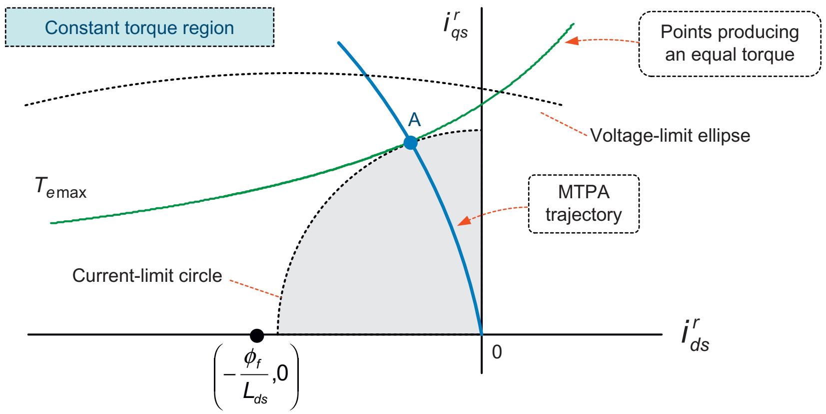

FIGURE 8.21

Current-limit circle and MTPA trajectory.

In the case of $\phi_f > L_{ds}I_{s\ max}$ it can be seen from Eq. (8.34) that there is a limitation on the operating speed at which the magnetic flux can be reduced by using the stator current, i.e., this type of motor has a *finite maximum speed*. On the other hand, in the case of $\phi_f < L_{ds}I_{s\ max}$, the maximum operating speed is theoretically infinite because the magnetic flux can be reduced fully by using the stator current, i.e., this type of motor has an *infinite maximum speed*. In this case, the operating speed is limited only by the mechanical strength. For these two cases, we need to use different flux-weakening control methods. First, let us take a look at the flux-weakening operation in the case of $\phi_f > L_{ds}I_{s\ max}$.

Fig. 8.21 illustrates numerous combinations of the current commands to produce an equal output torque, along with the voltage- and current-limit boundaries in the $d-q$ axes current plane.

In the low- and mid-speed range, the voltage-limit ellipse is large enough to encompass the current-limit circle. Thus we do not have to be concerned about the voltage-limit constraint, and the output torque depends only on the available current. In this case the optimal operating point is on the MTPA trajectory according to the given torque command. The maximum torque $T_{e\text{-}max}$ is produced at the intersection A of the current-limit circle and the MTPA trajectory. As the rotor speed increases, the boundary of the voltage-limit ellipse will be reduced. The boundary of the voltage-limit ellipse will encounter the MTPA operation point A at a specific speed as shown in Fig. 8.22. This specific speed is the base speed $\omega_{r\text{-}base}$ at which the flux-weakening control begins. When the operating speed is further increased above the base speed $\omega_{r\text{-}base}$, the voltage-limit ellipse shrinks more, so the operation point A will be outside the ellipse. As shown in Fig. 8.22, at speed $\omega_B(>\omega_{r\text{-}base})$, it can be readily seen that the currents at point A can be no longer regulated because it deviates from the region of controllable currents, i.e., the voltage is insufficient to regulate those currents.

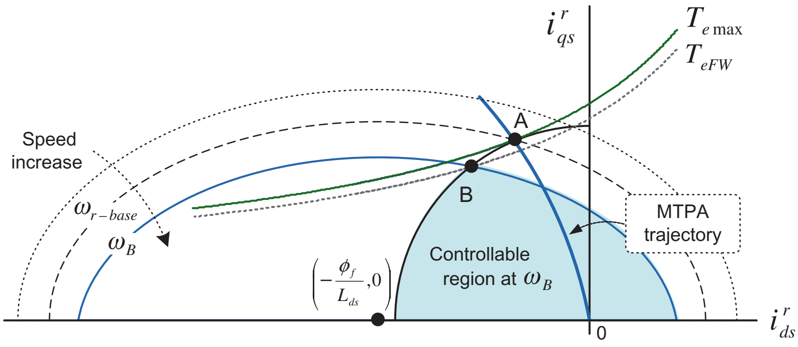

FIGURE 8.22

Onset of flux-weakening operation.

Thus the current command should be moved to the controllable operating point. Considering both the voltage-limit and the current-limit conditions, the optimal point for producing the maximum output torque is the intersection (point B) of the circle and the ellipse. The developed torque T_{eFW} at this point is less than the maximum torque $T_{e\text{-}max}$ in the constant torque region.

In such operation, the d-axis current increases in the negative direction. This is the flux-weakening control that reduces the effective stator flux linkage. The optimal $d-q$ axes currents for the stator current command I_s given as a torque command are expressed as

$$i_{ds}^r = \frac{L_{ds}\phi_f - \sqrt{(L_{ds}\phi_f)^2 + (L_{qs}^2 - L_{ds}^2)\left(\phi_f^2 + (L_{qs}I_s)^2 - \left(\frac{V_{s\,max}}{\omega_r}\right)^2\right)}}{(L_{qs}^2 - L_{ds}^2)} \tag{8.36}$$

$$i_{qs}^r = \sqrt{I_{s\,max}^2 - i_{ds}^{r*2}} \tag{8.37}$$

The trajectory of the optimal point moves along the current-limit boundary in a counterclockwise direction as the operating speed increases as shown in Fig. 8.23. Accordingly, the d-axis stator current increases in the negative direction while the q-axis stator current decreases.

This operation continues until $i_{ds}^{r*} = I_{s\,max}$ and $i_{qs}^{r*} = 0$, at which the operating speed reaches its maximum. Thus we can identify that this type of motor has a *finite maximum speed*. In such a flux-weakening operation, the stator voltage and current of an IPMSM remain constant, resulting in constant power operation. Fig. 8.24 shows the optimal currents in the flux-weakening operation of an IPMSM.

Next, let us take a look at the flux-weakening operation in the case of $\phi_f < L_{ds}I_{s\,max}$. In this case the center of the voltage-limit ellipse is inside the current-limit circle as shown in Fig. 8.25, and the trajectory of the optimal current is somewhat different from the case of $\phi_f > L_{ds}I_{s\,max}$. In the beginning of the flux-weakening operation, the trajectory of the optimal point moves along the

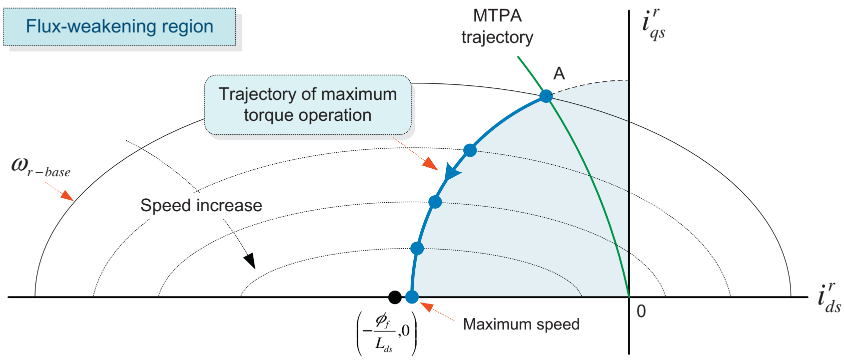

FIGURE 8.23

Optimal current vector in the flux-weakening operation ($\phi_f \geq L_{ds} I_{s\ max}$).

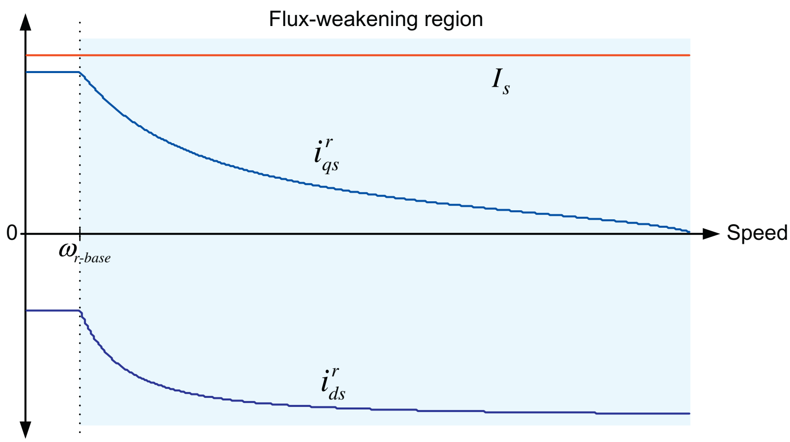

FIGURE 8.24

Optimal currents in the flux-weakening operation ($\phi_f > L_{ds} I_{s\ max}$).

current-limit boundary as the speed increases as in the case of $\phi_f > L_{ds} I_{s\ max}$. However, above a certain speed, the voltage-limit ellipse is gradually included in the current-limit circle. This means that the voltage-limit condition is included in the current-limit condition. If the optimal currents for the maximum torque subject to only the voltage-limit condition are included inside the current-limit circle (e.g., point C), then only the voltage-limit is the constraint that should be considered for obtaining the optimal currents. In this case the optimal point should move into the center of the ellipse as the speed increases instead of moving along the current-limit circle as shown in Fig. 8.25. Thus the optimal point is not point D, but point C. This flux-weakening operation is called as the MTPV (the maximum torque per voltage) operation. This operation region corresponds to the field-weakening region II of an induction motor.

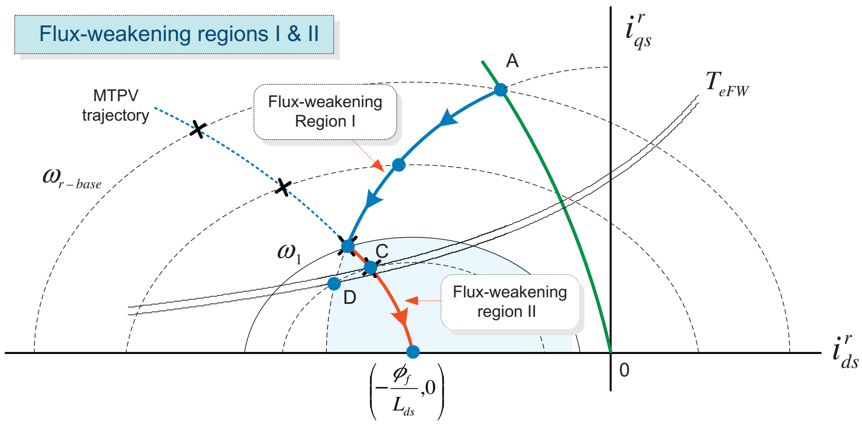

FIGURE 8.25

Optimal current trajectory in the flux-weakening region ($\phi_f < L_{ds} I_{s\ max}$)

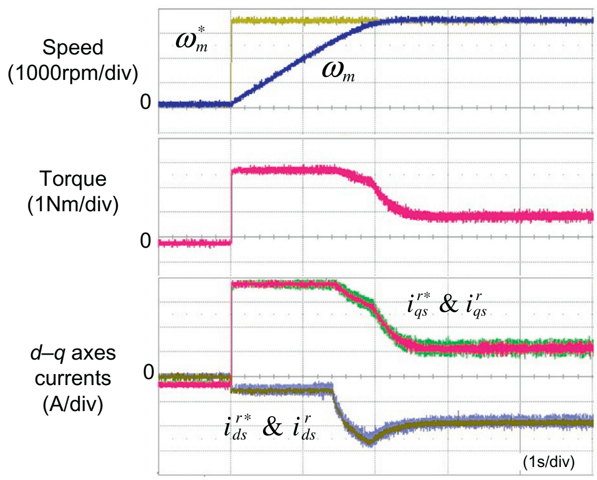

FIGURE 8.26

Flux-weakening operation of an 800-W IPMSM.

Fig. 8.26 shows the experimental results on the flux-weakening control for a 800-W, 8-pole IPMSM when the speed command is given as 3500 r/min. For this IPMSM, $\phi_f > L_{ds} I_{s\ max}$ and the base speed is 2500 r/min.

8.2.2 HIGH-SPEED OPERATION OF A SURFACE-MOUNTED PERMANENT MAGNET SYNCHRONOUS MOTOR

Unlike IPMSMs, the typical operating range of SPMSMs is the constant torque region. However, the high-speed operation of SPMSMs is often required in

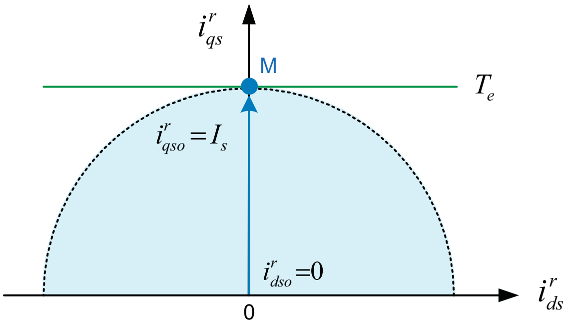

FIGURE 8.27

Optimal currents under the current-limit condition for an SPMSM.

several applications such as washing machines. The flux-weakening operation of SPMSMs is almost similar to that of IPMSMs. Now we will study the flux-weakening operation of SPMSMs. Similar to other motors, we will find out the optimal flux-weakening control method that ensures the maximum torque operation under the voltage- and the current-limit conditions.

The current-limit condition of an SPMSM is given as

$$i^{r2}_{ds} + i^{r2}_{qs} \leq I^2_{s\,max} \tag{8.38}$$

The current-limit boundary in the $d-q$ axes currents plane can be expressed as a circle whose radius is the maximum stator current $I_{s\,max}$ as shown in Fig. 8.27.

As stated in Section 5.5.1, for the MTPA operation of SPMSMs in the constant torque region, all the available current should be assigned to the q-axis stator current i^r_{qs} while making the d-axis stator current i^r_{ds} zero. Thus the optimal currents for the MTPA operation of the SPMSM under a given available stator current $I_{s\,max}$ become

$$i^{r*}_{dso} = 0 \tag{8.39}$$

$$i^{r*}_{qso} = I_{s\,max} \tag{8.40}$$

Fig. 8.27 depicts point M of the optimal currents under the current-limit condition. Similar to other motors, the possibility of the operation at this optimal point M depends on the following voltage-limit condition.

$$v^{r2}_{ds} + v^{r2}_{qs} \leq V^2_{s\,max} \tag{8.41}$$

For an SPMSM, neglecting the voltage drop of the stator resistance, from Eqs. (6.24) and (6.25), the steady-state $d-q$ axes voltage equations are expressed as

$$v^r_{ds} = -\,\omega_r L_s i^r_{qs} \tag{8.42}$$

$$v^r_{qs} = \omega_r (L_s i^r_{ds} + \phi_f) \tag{8.43}$$

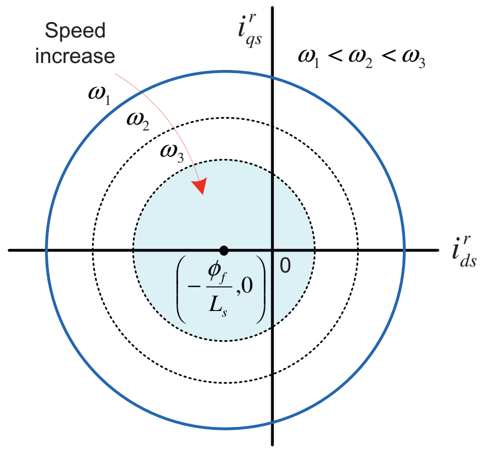

FIGURE 8.28

Voltage-limit condition for an SPMSM.

Thus the voltage-limit condition of Eq. (8.41) can be expressed from Eqs. (8.42) and (8.43) as

$$(\omega_r L_s i_{qs}^r)^2 + (\omega_r L_s i_{ds}^r + \omega_r \phi_f)^2 \le V_{s\,max}^2 \tag{8.44}$$

Unlike an IPMSM, the voltage-limit condition is expressed as a circle with the center $(-\phi_f/L_s, 0)$ in the $d-q$ axes currents plane as shown in Fig. 8.28. Under a given maximum stator voltage $V_{s\,max}$, the boundary of this circle becomes smaller as the operating speed increases.

The voltage- and current-limit conditions for a certain speed below the base speed are shown in Fig. 8.29. In this case, the optimal currents for producing the maximum torque (i.e., point M) are inside the voltage-limit circle, so they are controllable.

8.2.2.1 Constant power region $(\omega_e > \omega_{base})$

The voltage-limit circle dwindles with the increase in the speed. When point M begins to move out of the voltage-limit circle, the operating point should be changed. This indicates that the flux-weakening operation starts and the speed becomes the base speed.

In that case, the optimal point for producing the maximum output torque is the value at the intersection of two circles. From Eqs. (8.38) and (8.44), the optimal currents at this point are given as

$$i_{ds}^{r*} = \frac{\left(\frac{V_{s\,max}}{\omega_r}\right)^2 - \phi_f^2 - (L_s I_{s\,max})^2}{2L_s\phi_f} \tag{8.46}$$

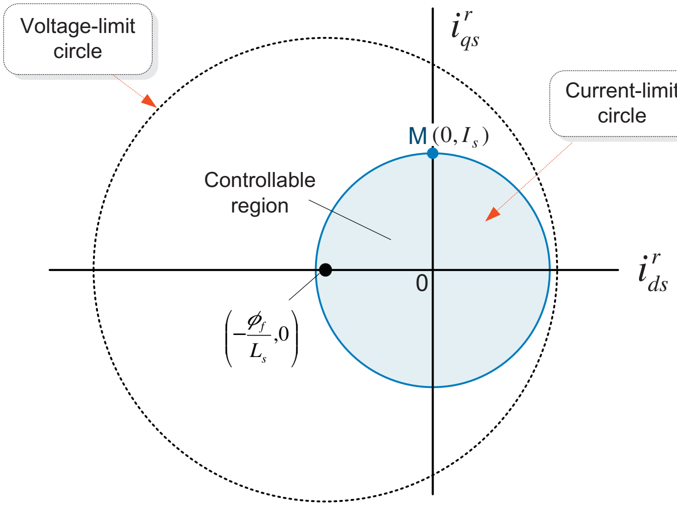

FIGURE 8.29

Voltage- and current-limit conditions for an SPMSM.

$$i_{qs}^{r*} = \sqrt{I_{s\,max}^2 - i_{ds}^{r*2}} \tag{8.47}$$

The trajectory of the optimal point moves along the current-limit boundary in a counterclockwise direction as the operating speed increases as shown in Fig. 8.30. Accordingly, the *d*-axis stator current increases in the negative direction while the *q*-axis stator current decreases.

Similar to an IPMSM, the maximum operating speed and the output power characteristic of an SPMSM vary according to the magnitude relationship between the magnet flux ϕ_f and the maximum *d*-axis stator flux linkage (i.e., $L_s I_{s\,max}$). In the case of $\phi_f > L_s I_{s\,max}$, the center of the voltage-limit circle is outside the current-limit circle, and there exists a limit on the operating speed (*finite maximum speed motor*). On the other hand, in the case of $\phi_f < L_s I_{s\,max}$, there is no limit on the maximum operating speed theoretically (*infinite maximum speed motor*) and also, there exists a speed range, which corresponds to the field-weakening region II of an induction motor. The optimal *d*-axis current of Eq. (8.46) corresponds to an SPMSM with $\phi_f > L_s I_{s\,max}$. This optimal *d*-axis current can be applied up to the maximum speed. The maximum operating speed is obtained when the *d*-axis current is equal to the stator maximum current, i.e., $i_{ds}^{r*} = I_{s\,max}$. However, in this case, the *q*-axis current becomes zero, so the maximum attainable speed will actually be less than that speed.

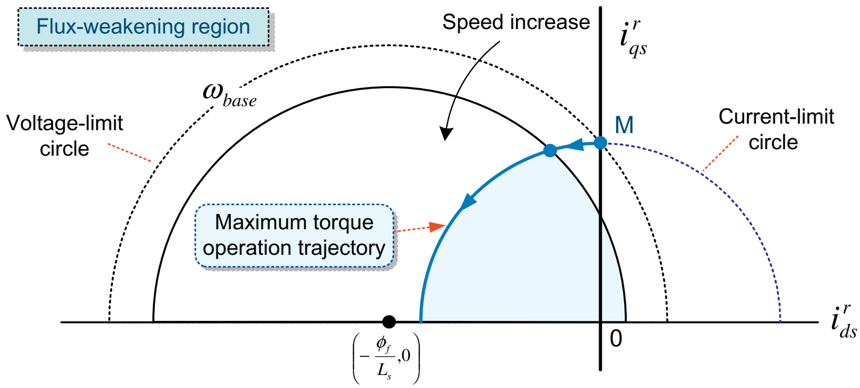

FIGURE 8.30

Trajectory of the optimal current vector (in case of $\phi_f > L_s I_{s\ max}$).

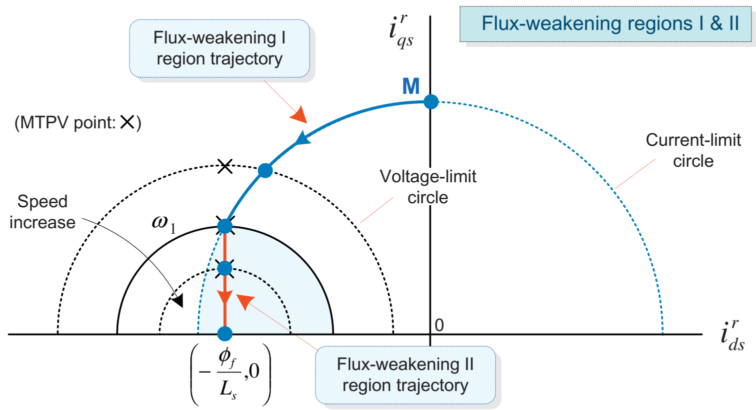

FIGURE 8.31

Trajectory of the optimal current vector (in case of $\phi_f < L_s I_{s\ max}$).

Next, we will discuss the case of $\phi_f < L_s I_{s\ max}$. In this case, the trajectory of the optimal current is identical to that in the case of $\phi_f > L_s I_{s\ max}$ in the beginning of the flux-weakening operation. However, if the optimal current for producing the maximum torque subject to only the voltage-limit constraint (the MTPV operation point X) is included inside the current-limit circle as shown in Fig. 8.31, then the MTPV operation needs to be carried out. In this operation, the d-axis stator current remains constant, while the q-axis stator current reduces as the speed increases.

REFERENCES

[1] S.-H. Kim, S.K. Sul, Maximum torque control of an induction machine in the field weakening region, IEEE Trans. Ind. Appl. 31 (4) (Jul./Aug. 1995) 787−794.

[2] S.-H. Kim, S.K. Sul, Voltage control strategy for maximum torque operation of an induction machine in the field-weakening region, IEEE Trans. Ind. Electron. 44 (4) (Aug. 1997) 512−518.

[3] J.M. Kim, S.K. Sul, Speed control of interior permanent magnet synchronous motor drive for the flux weakening operation, IEEE Trans. Ind. Appl. 33 (1) (Jan./Feb. 1997) 787−794.

[4] S.R. Macminn, T.M. Jahns, Control techniques for improved high-speed performance of interior PM synchronous motor drives, IEEE Trans. Ind. Appl. 27 (5) (Sep./Oct. 1991) 997−1004.

[5] T.S. Kwon, G.Y. Choi, M.S. Kwak, S.K. Sul, Novel flux-weakening control of an IPMSM for quasi-six-step operation, IEEE Trans. Ind. Appl. 27 (5) (Nov./Dec. 2008) 1722−1731.

[6] W.L. Soong, T.J.E. Miller, Field-weakening performance of brushless synchronous AC motor drives, IEE Proc. Elec. Power Appl. 141 (6) (Nov., 1994) 331−340.